# Time-Domain Distributed Fiber Sensor With 1 cm Spatial Resolution Based on Brillouin Dynamic Grating

Kwang Yong Song, Sanghoon Chin, Nikolay Primerov, and Luc Thévenaz

***Abstract*—We demonstrate an optical time-domain distributed fiber sensor showing the highest spatial resolution ever reported based on Brillouin dynamic grating in a polarization-maintaining fiber. In our scheme, the acoustic gratings containing the information on the local Brillouin frequency are generated by a long pump pulse in one polarization, and read out by a short probe pulse in the orthogonal polarization at a clearly distinct optical frequency from the pump. In the experiment, distributed temperature measurements over a 20 m fiber are performed with 1.2 cm spatial resolution.**

***Index Terms*—Brillouin scattering, gratings, optical fibers, optical fiber measurements.**

## I. Introduction

BRILLOUIN scattering in optical fibers has been studied over a couple of decades now as a useful sensing mechanism for distributed measurement of temperature or strain. Several measurement schemes have been developed to enlarge the measurement range, to improve the spatial resolution or to increase the measurement speed [1]–[5]. In Brillouin optical time-domain distributed sensors, the spatial resolution is determined by the duration of the pump pulse. However, this duration is practically limited to ~10 ns—equivalent to 1 m spatial resolution—since the broadening of the pump spectrum that results from a decreased pulse duration leads to a significant spectral spreading of the acquired Brillouin gain spectrum, hence causing a larger uncertainty in the determination of the Brillouin frequency $(\nu_B)$. In order to circumvent this resolution limit, a couple of innovative ideas have been proposed and experimentally demonstrated such as pre-generation of acoustic waves with pre-pulse or continuous wave pump [6], [7], use of a differential pulse-width pair [8], and Brillouin echoes [9]. However, the reported spatial resolutions were still limited to ~10 cm because the amplitude of the response was not sufficient for further improvement.

Manuscript received April 02, 2010; revised May 06, 2010; accepted May 11, 2010. Date of publication May 27, 2010; date of current version July 19, 2010. The work of K. Y. Song was supported by the National Research Foundation of Korea(NRF) grant funded by the Korea government (MEST) (No.2009-0068438).

The authors are with Ecole Polytechnique Fédérale de Lausanne, Institute of Electrical Engineering, 1015 Lausanne, Switzerland (e-mail: luc.thevenaz@epfl.ch).

Color versions of one or more of the figures in this paper are available online at http://ieeexplore.ieee.org.

Digital Object Identifier 10.1109/JLT.2010.2050763

Recently, the novel concept of Brillouin dynamic grating (BDG) has been reported using a polarization-maintaining fiber (PMF) [10], where acoustic waves generated during the process of stimulated Brillouin scattering (SBS) by optical waves (pump waves) in one polarization are used to reflect an orthogonally polarized wave (probe wave) at an optical frequency different from that of the pump. This phenomenon is called a 'dynamic' grating since the grating parameters such as the pitch and the reflectance are fully optically controllable by the pump waves. Among several reports on potential applications of BDGs [11]–[19], the feasibility study on a high resolution Brillouin optical time-domain analysis (BOTDA) has to be pointed out since it proposes another effective approach based on BDGs to improve the spatial resolution of ordinary BOTDA systems [18]. In this paper, we present an optimized experimental scheme to further improve the BDG-based BOTDA system and demonstrate a 1.2 cm spatial resolution in the distributed measurement of the Brillouin frequency along a 20 m PMF. To the best of our knowledge, this spatial resolution is the best result ever reported for time-domain Brillouin sensors, and almost an order of magnitude better than the former record.

## II. Principle

The operation principle of BDG is shown in Fig. 1, where the configurations of the propagation direction and the optical frequency $(\nu)$ correspond to the slow axis of the PMF set parallel to the $x$-axis. The two counter-propagating pump waves (Pump 1 and Pump 2) in $x$-polarization are spectrally positioned to interact in the ordinary way through stimulated Brillouin scattering. The acoustic wave mediating the interaction, generated through electrostriction by the interference of the two pump waves, is longitudinal and will therefore reflect indifferently light in any state of polarization, provided that this light satisfies the Bragg condition imposed by the periodic index perturbation induced by the acoustic wave. In isotropic conditions, such as in standard low birefringence fibers, the only waves satisfying this Bragg condition are the two counter-propagating interfering waves, resulting in a mutual energy transfer that globally results in a gain for the lower frequency wave though in-phase coupling and a loss for the upper frequency wave though $\pi$-phase coupling. The situation is fairly different in a birefringent medium, since the different refractive indexes for orthogonal eigenpolarizations result in a Bragg condition satisfied at a different frequency under the same spatial periodicity. This way it is possible to reflect a probe wave in the $y$-polarization on the periodic grating induced by the acoustic wave at an optical frequency

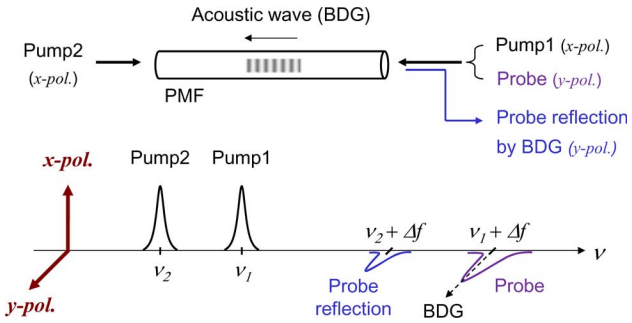


Fig. 1. Description of the concept for the generation and the reading of Brillouin dynamic grating.

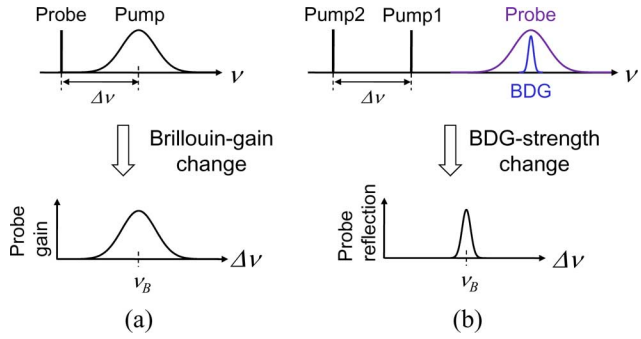


Fig. 2. Acquisition of a local Brillouin gain spectrum with a short pulse in (a) standard BOTDA systems by interrogation of the probe-gain variation, and (b) BDG-based BOTDA system by interrogation of the BDG-strength variation. $\nu_B$ indicates the local Brillouin frequency.

shifted by$\Delta f$ from Pump 1. This frequency shift $\Delta f$ linearly depends on the local birefringence $\Delta n$ through the following relation [10][17]:

$$\Delta f = \frac{\Delta n}{n_g}.\nu \tag{1}$$

where $n_g$and $\nu$ are the refractive index and the optical frequency of Pump 1, respectively. $\Delta f$ amounts to several ten's of GHz in most cases [10]–[19]. The benefit of this approach is to decouple the functions of generation and interrogation of the acoustic wave, its amplitude being probed by a distinct optical wave that is orthogonally polarized and well separated spectrally from the pumping wave, as sketched in Fig. 1.

In ordinary BOTDA systems, the measurement of the Brillouin gain spectrum (BGS) is carried out by sweeping the frequency offset $(\Delta\nu)$ between the pump and the probe waves as depicted in Fig. 2(a). The use of very short (< 10 ns) pump pulse results in the broadening of the acquired gain spectrum, which degrades the accuracy of the measurement. Such spectral broadening is attributed to the fact that the acquired gain spectrum corresponds to the convolution of the natural narrowband BGS with the normalized pump power spectrum [20].

Fig. 2(b) shows our scheme where the $x$-polarized pump waves generate the BDG interrogated by the $y$-polarized probe pulse. In this case, the amplitude of the probe reflection by the BDG is determined by the spectral overlap between the BDG and the probe pulse, and undoubtedly depends on the strength of the BDG which varies according to the frequency difference $\Delta\nu$ between the $x$-polarized pump waves. Thus, the shape of the BGS can be retrieved from the probe reflection by sweeping $\Delta\nu$ between Pump 1 and Pump 2. Since the spatial resolution of this measurement is determined by the duration of the probe pulse while the bandwidth of the Brillouin gain is related to the duration of Pump 1, a high spatial resolution BOTDA can be achieved while keeping a narrow effective BGS. Actually one can regard the BDG as a pure reflection or backscattering process, so the backscattered light can only come from the probe pulse and the spatial resolution is deduced following a similar approach to Rayleigh scattering in an OTDR system. It must be pointed out that the probe frequency is maintained fixed, since its spectrum covers a much broader spectrum than any reasonable variations of the BDG frequency resulting from environmental changes, as shown in Fig. 2(b).

It is worthwhile to comment on the bandwidth of the BDG and the amplitude of the BOTDA signal in this high-resolution measurement. The response of our system is given by the reflection of the probe pulse on the BDG, analogous to the pulse reflection on a fiber Bragg grating (FBG). Since the BDG is generated by a relatively long pump pulse (∼30 ns in our case), the effective length of the grating is ∼3 m corresponding to a spectral bandwidth of ∼20 MHz. However, when the length of the probe pulse is shorter than that of the BDG, the effective reflection bandwidth is increased and determined by the length of the probe pulse that delimits a short segment as effective for the reflection. Thus, there is no bandwidth limitation from the BDG when using a short (< 10 ns) probe pulse. Meanwhile, the reflectance of the BDG is function of the length of the probe pulse (i.e., the effective length of the grating), governed by the following equation for the case of a weak FBG [21]:

$$R = \tanh^2(\kappa L) \approx \kappa^2 L^2 \tag{2}$$

where $\kappa$ and $L$ are the strength and the length of the grating, respectively. Therefore, one can see that the amplitude of the BDG-based BOTDA signal is proportional to the squared spatial resolution in the high spatial resolution mode.

In the early experiment [18], a spatial resolution of 10 cm was reported, which was limited by the extinction ratio of an electro-optic modulator used to generate the probe pulse. This time we apply a gain-switching technique to a laser diode for generating an intense high-contrast ultra-short probe pulse (∼116 ps) and realize a 1.2 cm spatial resolution in the distributed measurement of the local BGS. The optimization of the filtering scheme and the control of the probe pulse spectrum are detailed hereafter.

## III. Experiments

The experimental setup is shown in Fig. 3, where two 1550 nm distributed feedback laser diodes (DFB LDs) were used for the pump and the probe waves, respectively. The sensing fiber (FUT) was a 20 m PMF with a Brillouin frequency $(\nu_B)$ of ∼10.82 GHz at the operating wavelength. The structure of the FUT is shown in the inset of Fig. 3, where two 1.5 cm sections within a 20 m PMF were temperature-controlled by a thermoelectric cooler (TEC). The output from the pump LD was divided by a 50/50 coupler, and Pump 1 was shaped as a 30 ns

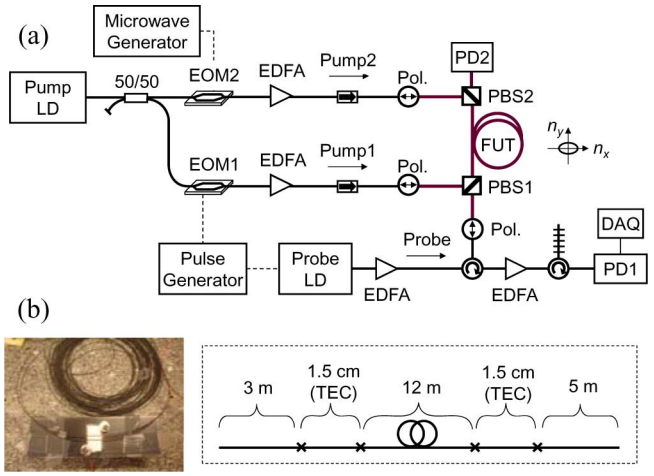


Fig. 3. (a) Experimental setup for the BDG-based BOTDA system: LD, laser diode; EDFA, Er-doped fiber amplifier; PBS, polarization beam splitter; Pol., fiber polarizer; EOM, electro-optic modulator; FUT, fiber under test; TEC, thermo-electric controller. (b) The photo and the structure of the FUT where two 1.5 cm sections were temperature-controlled by a TEC.

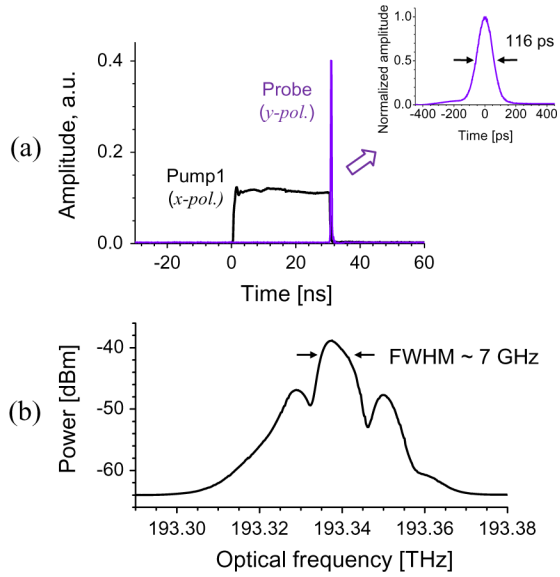


Fig. 4. (a) Timing and shape of the Pump 1 and the probe pulse. (b) Optical spectrum of the probe pulse.

square pulse at a 1 MHz repetition rate using a pulse generator and an electro-optic modulator (EOM1). Pump 2 was a continuous wave with the optical frequency down-shifted from Pump 1 to lie in the vicinity of $\nu_B$ of the PMF using a sideband-generation by another EOM (EOM2) and a microwave generator. Pump 1 and Pump 2 were prepared to counter-propagate along the slow axis ($x$-pol.) of the PMF using a fiber polarizer (Pol.) and fiber polarization beam splitters (PBS1 & PBS2) after being amplified by Er-doped fiber amplifiers (EDFAs) to 26 dBm and 14 dBm, respectively.

Pulsing Pump 1 makes possible to substantially raise its power without a massive transfer of power from Pump 1 to Pump 2, by limiting the interacting length between the two pumps. Such a transfer would eventually and substantially deplete Pump 1 and quench the generation of the acoustic wave after a few meters. It would also create a very uneven distribution of the pump powers along the fiber that would drastically distort the spectral information. On one hand Pump 1 pulse must be as short as possible to minimize these effects, but on the other hand it must be long enough to let the acoustic wave build up sufficiently. It was decided to fix the duration to 3 times the acoustic time response of 10 ns, so that the exponential growth of the acoustic wave reach some 95% of its asymptotic amplitude.

For the readout of the BDG, a 116 ps bell-shaped pulse was prepared as a probe using gain switching of the probe LD by direct current modulation through a pulse generator. The probe pulse was amplified by an EDFA and propagated in the same direction as Pump 1 along the fast axis ($y$-pol.) of the PMF through a polarization-maintaining (PM) circulator, a polarizer and PBS1 while the pump waves were propagated along the slow axis. The launch of the probe was synchronized to Pump 1 pulse so that the time delay between the probe and Pump 1 was set to 30 ns, the exact duration of Pump 1 (Pump 1 precedes). In this way, a strong BDG showing a narrow bandwidth is generated at the pumps crossing region and is always well-positioned to reflect the probe pulse along the fiber. The timing and the shapes of the pulses are depicted in Fig. 4(a) which was measured by PD2 shown in Fig. 3. The shaping of the optical spectrum of the probe pulse was carried out by controlling the width and the amplitude of the RF pulse, and Fig. 4(b) shows the best obtained spectrum used for the measurement, showing a 3-dB bandwidth of 7 GHz. It should be pointed out that this bandwidth corresponds to the coverage of a $> 140°$C temperature range according to the temperature sensitivity of the BDG spectrum [13].

The reflected signal from the BDG was extracted using a PM circulator and spectrally cleaned up by a tunable grating filter, before being pre-amplified by another EDFA prior to the detection by a 12 GHz photo diode (PD1) and the fast data acquisition (DAQ). Fig. 5 shows the optical spectrum measured in front of PD1 by an optical spectrum analyzer before (a) or after (b) applying the final EDFA and the tunable grating filter in Fig. 3. As depicted in Fig. 5(a), a strong reflection of the probe pulse from the BDG is clearly observed when Pump 1 is turned on, with a frequency offset $\Delta f$ of 44 GHz. The pump waves are also observed as a consequence of the finite extinction ratio ($\sim$20 dB) of the PM components. After applying the EDFA and the tunable filter, we could strongly attenuate the unnecessary frequency components while raising the reflected signal to a comfortable level for detection, as shown in Fig. 5(b). It is noteworthy that the power ratio of the signal and the other frequency components was maintained above 10 dB through the AC coupling of the PD1 to the DAQ.

We applied nominal temperature changes of $-5$, $+25$, $+50°$C to the TEC in contact with the sensing fiber, and performed distributed measurements by collecting the BDG reflection signal using PD2 while sweeping the frequency offset $\Delta\nu$ between Pump 1 and Pump 2 from 10.77 to 10.92 GHz. The raw traces were averaged 30 times and the accuracy in the $\nu_B$-determination was typically $\pm 1$ MHz. The measurement results are shown in Fig. 6 where the distribution of $\nu_B$ along the fiber is presented, showing clear shifts of $\nu_B$ at the positions of

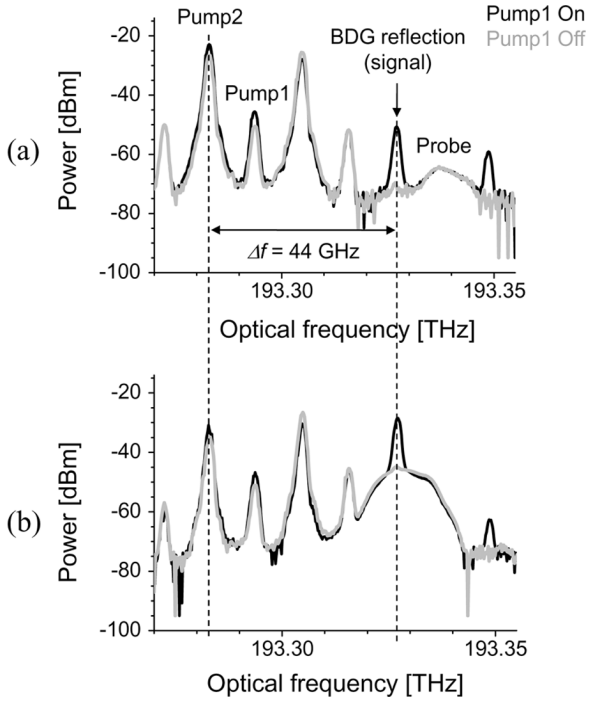


Fig. 5. Optical spectra measured in front of PD2 with Pump 1 on (black) and off (gray), before (a) and after (b) applying the EDFA and the tunable grating filter.

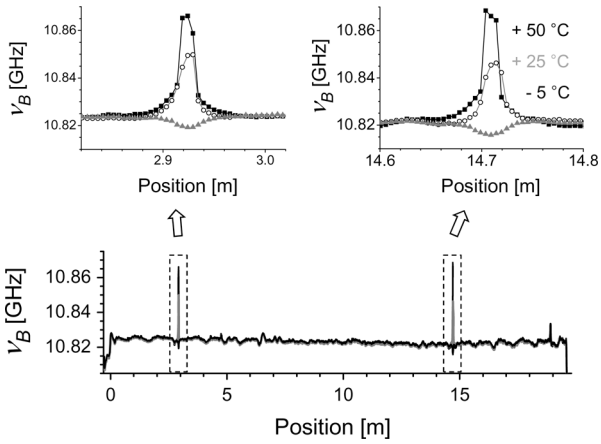


Fig. 6. Distribution of the Brillouin frequency $\nu_B$ along the fiber subject to 1.5 cm short temperature controlled sections acquired by the BDG-based BOTDA system (bottom) with the zoomed views of the dashed boxes (top).

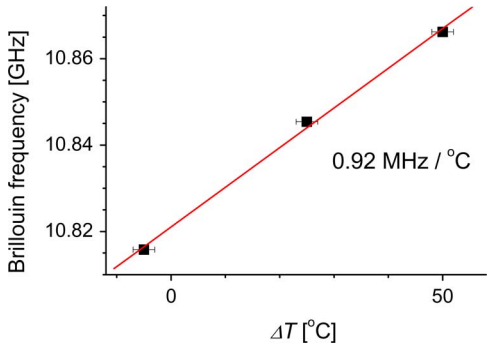


Fig. 7. Brillouin frequency shift as a function of temperature change $(\Delta T)$ at one of the TEC-applied sections (near the position of 14.7 m). The line is the result of a linear fit.

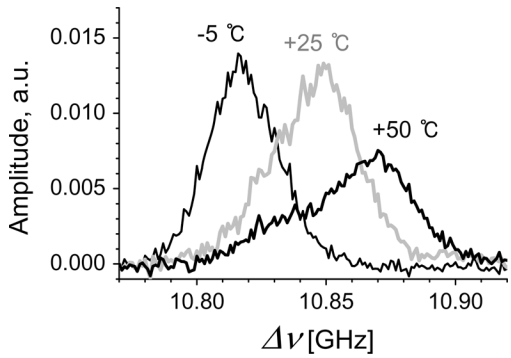


Fig. 8. Measured local BGS at one of the temperature-controlled sections (at position 14.7 m) for different temperature variations.

the TEC (bottom). The zoomed views of the temperature-controlled sections are depicted on top of Fig. 6, where the shifts of $\nu_B$ at the 1.5 cm sections were clearly detected, confirming the high resolution (∼1.2 cm) of the measurement. The relatively long transition extending over several centimeters between the heated segment and the rest of the fiber at ambient temperature does not result from an imperfectly resolved step transition, but simply from the normal heat conduction along the fiber. Using a simple heat transfer model the typical thermal diffusion length is calculated to be 3 cm in a 125 $\mu$m silica fiber, in perfect agreement with the measurement. It must be mentioned that the discreteness of the data points is due to the limited sampling rate of the DAQ (20 GSa/s, ∼2 pts/cm), and the small discrepancy (∼2 MHz) between the measurement results of two sections comes from the imperfect contact between the fiber and the TEC. Fig. 7 shows the Brillouin frequency shift as a function of temperature change $(\Delta T)$ at one of the TEC sections near the position of 14.7 m, which matches well to a line with a slope of 0.92 MHz/°C.

The local BGS in one of the TEC sections (near position 14.7 m) is depicted in Fig. 8, where one can see the clear shift of the BGS peak according to the temperature variation without apparent broadening of its spectrum. The width (FWHM) of the acquired BGS is remarkably maintained around 40–50 MHz. A decrease of the peak amplitude is also observed at $\Delta T = +50\,^{\circ}\mathrm{C}$, Which is due to the overall shift of the BDG spectrum by the temperature-dependence of the fiber birefringence. Actually a frequency shift of about 2.5 GHz is expected considering the overall temperature dependence (∼ 50 MHz/°C) of the BDG frequency [12]. Therefore, the observed amplitude drop of about 50% is well explained considering the spectral width (∼7 GHz) of our probe pulse (see Fig. 4(b)). This feature results in a variation of the reflectance, however it does not affect the accuracy of the measurement but only the amplitude of the signal [18].

Fig. 9 shows 3-D Brillouin gain spectra constructed from the measured local BGS near one of the TEC positions, where the local shift of the gain peak is clearly seen for each $\Delta T$.

## IV. Summary

We have demonstrated a high resolution BOTDA system based on the BDG in a polarization-maintaining fiber, where

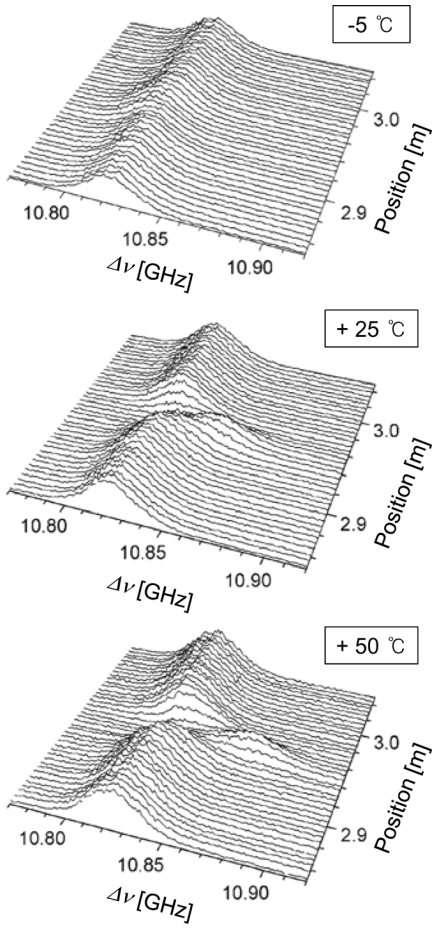


Fig. 9. 3-D plots of distributed Brillouin gain spectra near one of the temperature-controlled sections with $\Delta T = -5, +25$ and $+50$°C, respectively. Note that each time trace was averaged only 30 times.

the local BDG is exploited to reflect the probe waves. To the best of our knowledge, 1 cm spatial resolution was for the first time realized in a pulse-based Brillouin sensor. This result is certainly not the ultimate limit, and the broadening of pulse spectrum is no longer the dominant cause limiting spatial resolution. We believe further investigation is necessary to find out what limits the spatial resolution in the presented scheme. This result proves that our novel approach opens unprecedented perspectives for distributed fiber sensing, combining a simple principle giving a clean spectral response to a potentially unlimited spatial resolving power. Segments of the size of a classical Bragg grating can be dynamically addressed at any position along the fiber, offering flexibility about the reconfiguration of the sensor that a fixed Bragg grating cannot offer. The sensing range can be certainly expanded to 100 m, but a kilometer range remains highly questionable, since the polarization is unlikely to be maintained over this distance and the critical power for amplified spontaneous scattering will probably be reached for the continuous Pump 2. The 20 m tested range already offers 2000 resolved points, performance that remain challenging and complex using alternative techniques with comparable spatial resolutions, such as multiplexed fiber Bragg gratings or the Brillouin optical-correlation domain analysis.

## REFERENCES

[1] X. Bao, D. J. Webb, and D. A. Jackson, "32-km distributed temperature sensor using brillouin loss in optical fiber," *Opt. Lett.*, vol. 18, pp. 1561–1563, 1993.

[2] M. Nikles, L. Thevenaz, and P. A. Robert, "Brillouin gain spectrum characterization in single-mode optical fibers," *J. Lightw. Technol.*, vol. 15, no. 10, pp. 1842–1851, Oct. 1997.

[3] K. Hotate and T. Hasegawa, "Measurement of Brillouin gain spectrum distribution along an optical fiber using a correlation-based technique—proposal, experiment and simulation," *IEICE Trans. Electron.*, vol. E83-C, pp. 405–412, 2000.

[4] M. N. Alahbabi, Y. T. Cho, and T. P. Newson, "150-km-range distributed temperature sensor based on coherent detection of spontaneous Brillouin backscatter and in-line Raman amplification," *J. Opt. Soc. Amer. B*, vol. 22, pp. 1321–1324, 2005.

[5] K. Y. Song, Z. He, and K. Hotate, "Distributed strain measurement with millimeter-order spatial resolution based on Brillouin optical correlation domain analysis," *Opt. Lett.*, vol. 31, pp. 2526–2528, 2006.

[6] L. Che-Hien, T. Tsuda, and K. Kishida, "PPP-BOTDA Method to Achieve cm-Order Spatial Resolution in Brillouin Distributed Measuring Technique," IEICE Technical Report, Aug. 2005, OFT 2005-16.

[7] V. P. Kalosha, E. A. Ponomarev, L. Chen, and X. Bao, "How to obtain high spectral resolution of SBS-based distributed sensing by using nanosecond pulses," *Opt. Exp.*, vol. 14, pp. 2071–2078, 2006.

[8] W. Li, X. Bao, Y. Li, and L. Chen, "Differential pulse-width pair BOTDA for high spatial resolution sensing," *Opt. Exp.*, vol. 16, pp. 21616–21625, 2008.

[9] S. Foaleng-Mafang, J. C. Beugnot, and L. Thevenaz, "Optimized configuration for high-resolution distributed sensing using Brillouin echoes," in *Proc. SPIE*, 2009, vol. 7503, pp. 75032C–.

[10] K. Y. Song, W. Zou, Z. He, and K. Hotate, "All-optical dynamic grating generation based on Brillouin scattering in polarization maintaining fiber," *Opt. Lett.*, vol. 33, pp. 926–928, 2008.

[11] V. P. Kalosha, W. Li, F. Wang, L. Chen, and X. Bao, "Frequency-shifted light storage via stimulated Brillouin scattering in optical fibers," *Opt. Lett.*, vol. 33, pp. 2848–2850, 2008.

[12] W. Zou, Z. He, K. Y. Song, and K. Hotate, "Correlation-based distributed measurement of a dynamic grating spectrum generated in stimulated Brillouin scattering in a polarization-maintaining optical fiber," *Opt. Lett.*, vol. 34, pp. 1126–1128, 2009.

[13] K. Y. Song, W. Zou, Z. He, and K. Hotate, "Optical time-domain measurement of Brillouin dynamic grating spectrum in a polarization maintaining fiber," *Opt. Lett.*, vol. 34, pp. 1381–1383, 2009.

[14] W. Zou, Z. He, and K. Hotate, "Complete discrimination of strain and temperature using Brillouin frequency shift and birefringence in a polarization-maintaining fiber," *Opt. Exp.*, vol. 17, pp. 1248–1255, 2009.

[15] K. Y. Song, K. Lee, and S. B. Lee, "Tunable optical time delays based on Brillouin dynamic grating in optical fibers," *Opt. Express*, vol. 17, pp. 10344–10349, 2009.

[16] Y. Dong, X. Bao, and L. Chen, "Distributed temperature sensing based on birefringence effect on transient Brillouin grating in a polarization-maintaining photonic crystal fiber," *Opt. Lett.*, vol. 34, pp. 2590–2592, 2009.

[17] Y. Dong, L. Chen, and X. Bao, "Truly distributed birefringence measurement of polarization-maintaining fibers based on transient Brillouin grating," *Opt. Lett.*, vol. 35, pp. 193–195, 2010.

[18] K. Y. Song and H. J. Yoon, "High-resolution Brillouin optical time domain analysis based on Brillouin dynamic grating," *Opt. Lett.*, vol. 35, pp. 52–54, 2010.

[19] N. Primerov, S. Chin, K. Y. Song, and L. Thevenaz, "Ultra wide range tunable delay line using dynamic grating reflectors in optical fibers," in *Proc. OFC 2010*, Paper OWF6.

[20] E. Lichtman, R. G. Waarts, and A. A. Friesem, "Stimulated Brillouin scattering excited by a modulated pump wave in single-mode fibers," *J. Lightw. Technol.*, vol. 7, no. 1, pp. 171–174, Jan. 1989.

[21] T. Erdogan, "Fiber grating spectra," *J. Lightw. Technol.*, vol. 15, no. 8, pp. 1277–1294, Aug. 1997.

**Kwang Yong Song** received the Ph.D. degree in physics from Korea Advanced Institute of Science and Technology (KAIST) in 2003.

From 2003, he worked as a post-doctoral researcher in KAIST and then moved to the Nanophotonics and Metrology Laboratory in the Ecole Polytechnique Federale de Lausanne (EPFL), Switzerland, where he performed researches on the applications of Brillouin scattering in optical fibers. In 2005, he joined in the Department of Electronic Engineering, University of Tokyo as a Research Fellow. In 2007, he became an Assistant Professor in Department of Physics, Chung-Ang University in South Korea. His current research interests are the applications of Brillouin scattering in optical fibers including Brillouin slow light, Brillouin dynamic grating and Brillouin distributed sensors.

**Sanghoon Chin** received the M.S. degree in information and communication from Gwangju Institute of Science and Technology (GIST), South Korea, in 2005. In 2009, he received the Ph.D. degree in electrical engineering department from Ecole Polytechnique Fédérale de Lausanne (EPFL), Switzerland, where he developed his expertise on slow and fast light.

His research was mainly oriented to progress the dynamic control of speed of a light signal in optical fibers, using stimulated Brillouin scattering in fibers. After receiving the Ph.D., he has been working as Postdoctoral Researcher in EPFL. In 2010, He got academic visits in Polytechnique University in Valencia, Spain, and in Thales Research & Technology, Palaiseau, France, respectively and improved his expertise on broadband microwave signal processing based on photonic delay line.

**Nikolay Primerov,** photograph and biography unavailable at time of publication.

**Luc Thévenaz** received the M.Sc. degree in 1982 and the Ph.D. degree in physics in 1988, both from the University of Geneva, Switzerland.

In 1988 he joined the Swiss Federal Institute of Technology of Lausanne (EPFL) where he currently leads a research group involved in photonics, namely fiber optics and optical sensing. Research topics include Brillouin-scattering fiber sensors, slow and fast light, nonlinear fiber optics and laser spectroscopy in gases. He achieved with his collaborators the first experimental demonstration of optically controlled slow and fast light in optical fibers, and is at the origin of innovative configurations for Brillouin distributed fiber sensors, such as generation of the signal wave using modulation sidebands and Brillouin dynamic gratings. During his career he stayed at Stanford University, at the Korea Advanced Institute of Science and Technology (KAIST), at Tel Aviv University and at the University of Sydney. In 2000 he co-founded the company Omnisens that is developing and commercializing advanced photonic instrumentation.

Prof. Thévenaz is Chairman of the European COST Action 299 "FIDES: Optical Fibres for New Challenges Facing the Information Society" and author or coauthor of some 280 publications and 5 patents.